Dalton Transactions

Cite this: *Dalton Trans.*, 2012, **41**, 953

www.rsc.org/dalton

PAPER

Zinc and magnesium complexes incorporated by bis(amine) benzotriazole phenoxide ligand: Synthesis, characterization, photoluminescent properties and catalysis for ring-opening polymerization of lactide†

Chang-Yu Sung, Chen-Yu Li, Jing-Kai Su, Ting-Yi Chen, Chia-Her Lin and Bao-Tsan Ko*

Received 3rd August 2011, Accepted 4th October 2011
DOI: 10.1039/c1dt11461a

A new bis(amine) benzotriazole phenoxide ligand, ^{C8NN}**BTP**-H (**1**) was prepared from the Mannich condensation of 2-(2*H*-benzotriazol-2-yl)-4-(2,4,4-trimethylpentan-2-yl)phenol with the mixtures of excess paraformaldehyde and N,N,N-trimethylethylenediamine under reflux conditions. Zinc and magnesium complexes bearing the N,N,O-tridentate ^{C8NN}**BTP** ligand were synthesized and fully characterized. The reaction of ^{C8NN}**BTP**-H with $ZnEt_2$ (1.2 molar equiv.) in toluene gives the monomeric tetra-coordinated zinc complex [(^{C8NN}**BTP**)ZnEt] (**2**). The homoleptic and monomeric complexes [(^{C8NN}**BTP**)$_2$M] (M = Zn (**3**) and M = Mg (**4**)) result from treatment of $ZnEt_2$ or Mg^nBu_2 with ^{C8NN}**BTP**-H (two equiv.), in which the metal center is hexa-coordinated by two tridentate ^{C8NN}**BTP** ligands. Luminescent properties and catalysis for lactide (LA) polymerizations of complexes **2–4** are studied. Complexes **2–4** produce bright green fluorescence with emission maxima ranging from 510 to 520 nm in the solid state. Experimental results indicate that complex **2** catalyzes the ring-opening polymerization of LA in the presence of 9-anthracenemethanol (9-AnOH) with efficient catalytic activities in a controlled fashion, yielding poly(rac-lactide) with a slight isotactic predominance (P_m = 0.59).

Introduction

The development of catalytic systems for the ring-opening polymerization (ROP) has attracted considerable attention in recent years. ROP using well-defined metal complexes provides a promising method to prepare biodegradable polymers such as poly(ε-caprolactone) (PCL), poly(lactide) (PLA) and poly(3-hydroxybutyrate) (PHB) with controlled molecular weights and narrow distributions. Among them, metal complexes with a so-called single active site supported by various ancillary ligands such as β-diketiminate, Schiff base, amino-bis(phenolate), bisphenolate[1] and anilido-aldiminate[2] have been reported to achieve great catalytic activities in a controlled manner. Particularly, metal complexes bearing phenolate ligands containing nitrogen donors are receiving increasing attention due to the successful catalytic systems of metal phenoxyimine and phenoxyamine complexes in the ROP.[3] Their metal complexes of aluminium, calcium, lithium, magnesium, zinc and yttrium have shown to be effective catalysts for ROP of cyclic esters. For instance, N,N,O-tridentate Schiff-base magnesium and zinc alkoxides are demonstrated to be excellent initiators toward the controlled polymerization of L-lactide (L-LA), and their activities are greatly dependent on the electronic effect of the substituents on the Schiff-base ligands.[4]

Recently, we have investigated the synthesis and catalysis of well-characterized aluminium and zinc complexes derived from the N,O-bidentate benzotriazole phenoxide (**BTP**) ligands (type **I**, Chart 1).[5] The zinc complexes have been demonstrated to efficiently catalyze the ROP not only by using ε-caprolactone (ε-CL) as monomers but also by using β-butyrolactone (β-BL) as monomers, giving polymers with the expected molecular weights and very narrow PDIs (≦1.10). On the basis of the excellent catalytic systems supported by **BTP** ligands, our current interest has been to develop amino- or imine-**BTP** ligands[6] incorporating aluminium, magnesium and zinc derivatives and to apply these complexes as catalysts for CO_2/epoxide coupling and ROP of cyclic esters. For instance, amino-benzotriazole phenol derivatives (type **II**, Chart 1) are successfully prepared by one-pot Mannich condensation, and zinc complexes bearing such ligands catalyze the ROP of ε-CL and β-BL with good catalytic activities in a controlled fashion.[7] To extend studies for amino-**BTP**

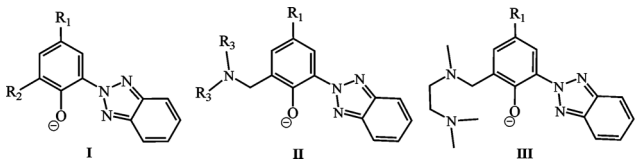

Chart 1 Types of benzotriazole phenoxide (**BTP**) derivatives.

Department of Chemistry, Chung Yuan Christian University, Chung-Li, 32023, Taiwan. E-mail: btko@cycu.edu.tw; Fax: 886-3-2653399; Tel: 886-3-2653327

† CCDC reference numbers 837485–837491. For crystallographic data in CIF or other electronic format see DOI: 10.1039/c1dt11461a

derivatives and to achieve the criteria of single-site catalysts, a novel bis(amine) benzotriazole phenoxide ligand (type **III**, Chart 1) has been designed and synthesized. We envisaged that the additional bis(amine) group can provide the better chelation to stabilize the metal center to realize mononuclear complexes. Moreover, **BTP** derivatives are widely used as ultraviolet (UV) absorbers for the protection of commercially important synthetic resins against the UV light in industrial applications.[8] It is therefore interesting to explore the photoluminescent behaviors of amino-**BTP** incorporating metal complexes. Herein, we describe the synthesis, structure, optical properties, and LA polymerization catalytic studies of zinc and magnesium derivatives based on the amino-**BTP** ligand of this kind.

Results and discussion

Syntheses and crystal structure

The synthetic routes of bis(amine) benzotriazole phenol ligand (^{C8NN}**BTP**-H, **1**) and their Zn and Mg complexes **2–4** are shown in Scheme 1. The bis(amine)-**BTP**-H derivative was prepared in 71% yield from the reaction of 2-(2*H*-benzotriazol-2-yl)-4-(2,4,4-trimethylpentan-2-yl)phenol (^{C8}**BTP**-H) with the mixtures of paraformaldehyde (4 molar equiv.) and N,N,N-trimethylethylenediamine (4 equiv.), in the absence of solvent, under reflux. The novel ligand (^{C8NN}**BTP**-H) was isolated as yellow solids and easily purified by recrystallization from hexane solution. It was also characterized by spectroscopic studies as well as microanalyses. For instance, the ^{1}H NMR spectrum of the ligand displayed resonances about δ 3.78 ppm for the methylene protons of -CH_2N~NMe$_2$, and signals of methyl (δ = 2.32 ppm, 3H) and methylene (δ = 2.62 and 2.51 ppm, 2H each) protons of –N(CH_3)–CH_2CH_2NMe$_2$, indicating the formation of the expected ^{C8NN}**BTP**-H ligand. The broad O–H signal for ^{C8NN}**BTP**–H at the downfield of 10.92 ppm implied a hydrogen bond between O–H and N (–CH$_2$N~*N*Me$_2$), which was further confirmed by X-ray structural determination. Complexes **2–4** were synthesized *via* alkane elimination in toluene. The tetra-coordinated mono-adduct zinc complex [(^{C8NN}**BTP**)ZnEt] (**2**) was synthesized in 67% yield on the reaction of ^{C8NN}**BTP**–H with ZnEt$_2$ (1.2 molar equiv.) in toluene. The formation of the expected Zn–Et complex **2** was demonstrated by the disappearance of the O–H signal (~10.9 ppm) of ^{C8NN}**BTP**-H and the appearance of resonances for methylene (δ = 0.06 ppm, 2H) and methyl (δ = 1.15 ppm, 3H) protons of ethyl group bound to the zinc atom in the ^{1}H NMR spectrum. Furthermore, treatment of ^{C8NN}**BTP**-H (two equiv.) with ZnEt$_2$ in toluene at 50 °C gave the six-coordinated bis-adduct zinc complex [(^{C8NN}**BTP**)$_2$Zn] (**3**). The NMR spectra of complex **3** exhibited broad resonances for ligand signals at 20 °C, and we could not make reasonable assignments for these spectral data. This may be attributed to the existence of fluxional behaviors between isomers in solution. The homoleptic magnesium complex [(^{C8NN}**BTP**)$_2$Mg] (**4**) was prepared in high yield (80%) by using Mg^{n}Bu$_2$ as the metal precursor according to the same synthetic route, but the reaction was carried out at 25 °C. The NMR spectra of complex **4** showed one set of ligand signals, which proved that two ligands adopted the same coordination mode. Attempts to isolate the mono-adduct magnesium complex modified with the ^{C8NN}**BTP**$^-$ ligand were unsuccessful. To obtain reasonable assignments for Zn complex **3**, variable temperature NMR studies were performed.

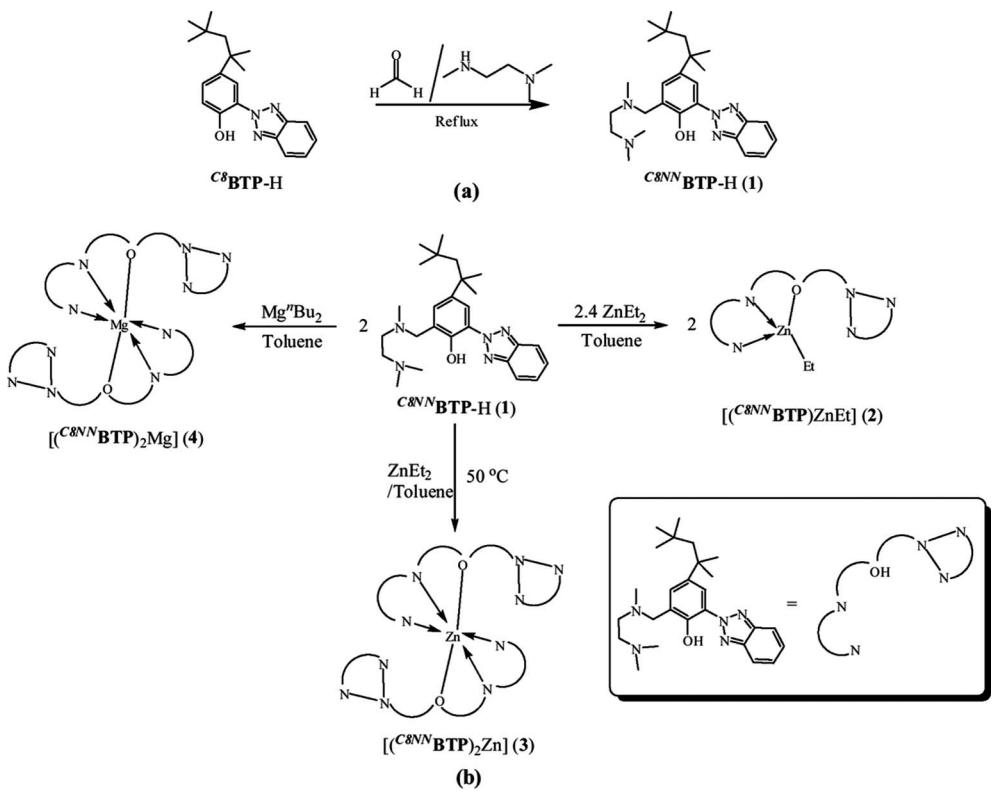

Scheme 1 Synthetic routes of (a) ligand ^{C8NN}**BTP**-H (**1**) and (b) complexes (**2**)–(**4**).

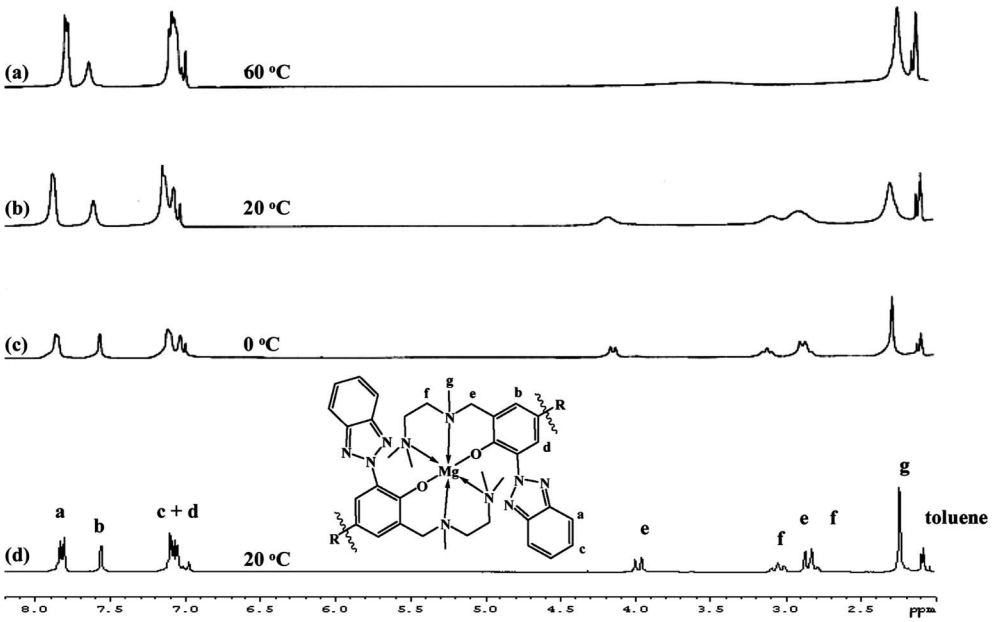

Fig. 1 Variable-temperature ^{1}H NMR spectrum (400 MHz) of [(^{C8NN}**BTP**)$_2$Zn] (**3**) in d_8-toluene taken at different temperatures: (a) 60 °C; (b) 20 °C; (c) 0 °C, and (d) ^{1}H NMR spectrum of [(^{C8NN}**BTP**)$_2$Mg] (**4**) at 20 °C in d_8-toluene.

The ^{1}H NMR spectra of **3** (Fig. 1) in d_8-toluene at 60 °C and 20 °C all show broad resonance peaks. While the temperature decreases from 20 to 0 °C, signals of the ^{C8NN}**BTP**–H ligand become sharp and show one set of resonance peaks. In addition, these peaks exhibit similar resonance patterns in comparison with those of isostructural Mg complex **4** as shown in Fig. 1(d). Complexes **2–4** were isolated as yellow crystalline solids and were characterized by microanalyses as well as X-ray single crystal measurements.

Single crystals suitable for X-ray structural analysis of ^{C8NN}**BTP**-H (**1**) were obtained from a saturated hexane solution. The molecular structure of compound **1** (Fig. 2) shows an intramolecular hydrogen bond of O–H···N between the phenol and dimethylamine group of N,N-pendant arm. The distance of N···H (1.881(3) Å) is substantially shorter than the Van der Waals distance of 2.75 Å for the N and H atom, and the angle (O–H(1)···N(5)) formed by the hydrogen bond is 157.4 (2)°. The dihedral angle between the planes of the phenyl ring of the phenolate group and the benzotriazole unit is 101.2 (2)°. It is worthy of note that the intramolecular hydrogen bond for ^{C8NN}**BTP**–H is similar to that for ^{C8DEA}**BTP**–H reported in our earlier studies.[7] Single crystals of complexes **2–4** suitable for X-ray structural determinations were grown from their saturated Et_2O solutions. Oak Ridge Thermal Ellipsoid Plot (ORTEP) drawings illustrating selected bond distances and angles of the molecular structures of **2**, **3** and **4** are shown in Fig. 3, 4 and 5, respectively. Complex **2** shows a monomeric feature with a four-coordinated Zn center, containing one six- and one five-membered chelating ring. The six-membered ring, consisting of a Zn coordinated with the phenoxy oxygen atom and amine nitrogen atom of the ^{C8NN}**BTP**$^-$ ligand, is not planar, showing a twist conformation. All the bond angles around Zn in **2**, in a range 83.34(8)–126.22(9)°, display a distorted tetrahedral geometry. The distances between the Zn atom and atoms O, N(4), N(5) and C(27) are 1.9447(16), 2.1507(19), 2.155(2) and 1.983(2) Å, respectively. These distances are all comparable with bond lengths observed

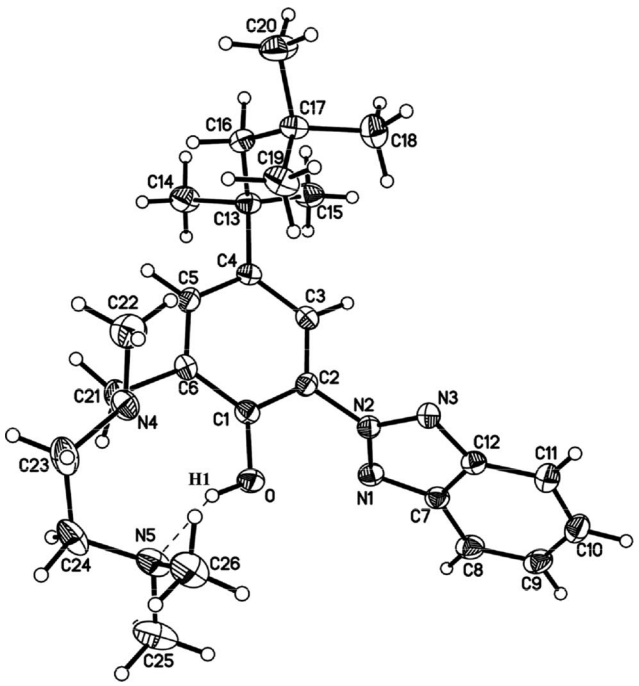

Fig. 2 ORTEP drawing of ^{C8NN}**BTP**–H (**1**) with probability ellipsoids drawn at the 60% level. Selected bond lengths (Å) and angles (deg): N(1)–N(2) 1.3311(18), N(2)–N(3) 1.3308(18), N(2)–C(2) 1.4375(19), C(6)–C(21) 1.504(2), N(4)–C(21) 1.464(2), N(4)–C(22) 1.455(2), N(4)–C(23) 1.460(2), N(4)···H(1) 1.881(3), O–H(1)···N(5) 157.4 (2).

for the monomeric zinc complexes containing the N,N,O-amine phenolate derivative.[3b,l]

The molecular structures of complexes **3** and **4** are isostructural, except either the zinc or magnesium atom is the metal center. Both crystallize in monoclinic space group $C2/c$ with one half

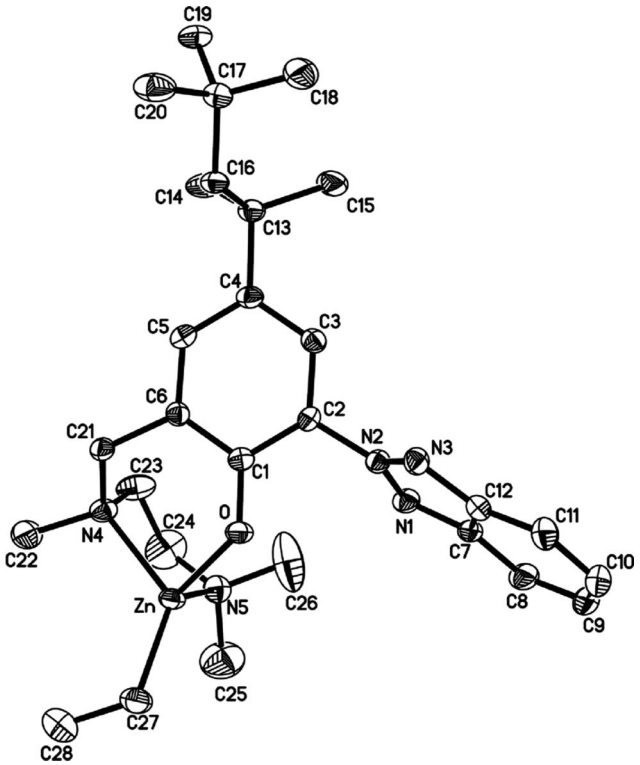

Fig. 3 ORTEP drawing of complex **2** with probability ellipsoids drawn at the 60% level. Hydrogen atoms are omitted for clarity. Selected bond lengths (Å) and angles (deg): Zn–O 1.9447(16), Zn–N(4) 2.1507(19), Zn–N(5) 2.155(2), Zn–C(27) 1.983(2), O–Zn–N(4) 93.06(7), O–Zn–N(5) 100.79(7), N(4)–Zn–N(5) 84.34(8), O---Zn–C(27) 126.22(9), N(4)–Zn–C(27) 125.46(10), N(5)–Zn–C(27) 117.22(10).

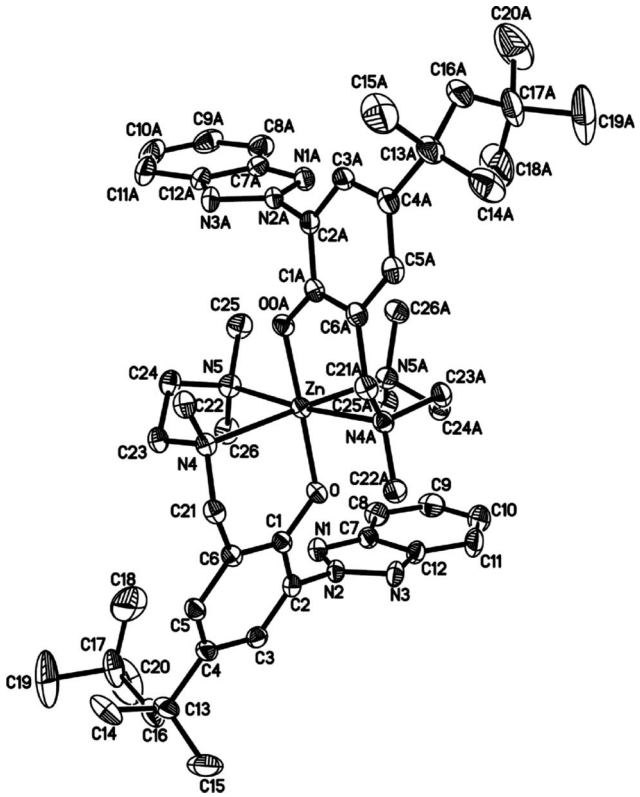

Fig. 4 ORTEP drawing of complex **3** with probability ellipsoids drawn at the 50% level. Hydrogen atoms are omitted for clarity. Selected bond lengths (Å) and angles (deg): Zn–O 1.9535(10), Zn–N(4) 2.3569(12), Zn–N(5) 2.2993(12), O–Zn–O(0A) 172.30(6), O–Zn–N(5A) 88.59(4), O(0A)–Zn–N(5A) 96.49(4), N(5A)–Zn–N(5) 97.60(6), O–Zn–N(4) 87.88(4), O(0A)–Zn–N(4) 87.47(4), N(5A)–Zn–N(4) 174.46(4), N(5)–Zn–N(4) 78.57(4), N(5)–Zn–N(4A) 174.46(4), N(4)–Zn–N(4A) 105.53(6).

of **3** and **4** in the asymmetric unit. The solid structure of **3** or **4** reveals also a monomeric M^{II} (M = Zn or Mg) complex that contains two ^{C8NN}**BTP**$^-$ ligands. The geometry around the Zn or Mg center is hexa-coordinated with a slightly distorted octahedral environment. Their principal structural features include four nitrogen atoms (N(4), N(5), N(4A), N(5A)) from two ^{C8NN}**BTP**$^-$ ligands occupying the equatorial plane; the angles O–Zn–O(0A) and O–Mg–O(0A) formed by the axial bonds are 172.30(6)° and 171.47(17)°, respectively. The average bond distances between the Zn atom and O(phenoxy) and N(amine) are, respectively, 1.9535(10) and 2.3281(12) Å for **3**, which are longer than the bond lengths observed for four-coordinated Zn complex **2**. Relative to Zn complex **3**, the average Mg–O(phenoxy) covalent bond distance (1.929(3) Å) for **4** is shorter, which is probably due to the higher Lewis acidity and oxophilic nature of the Mg^{2+} atom. However, the average Mg–N(amine) distance (2.330(3) Å) in **4** is similar to that of bis-adduct Zn analogue **3**. It is interesting to note that all ^{C8NN}**BTP**$^-$ ligands in complexes **2–4** assume N,N,O-tridentate bonding mode to coordinate the metal centers.

Optical properties

To examine the optical properties of amino-**BTP** containing derivatives **1–4**, UV/Vis and photoluminescence (PL) experiments were performed. The absorption (left) and emission (right) spectra of compounds **1–4** in dichloromethane (CH_2Cl_2) are shown in Fig. 6, and the corresponding maximum absorption and emission wavelengths (λ_{max}) characterized in both solution and the solid state are summarized in Table 1. The major absorption bands of compounds **1–4** are all around at 243–289 nm and 333–346 nm, which can be assigned to intraligand π–π* and n–π* transitions. The dilute concentrations (5×10^{-5} M) of those compounds in CH_2Cl_2 are conducted to be the same and their absorption coefficient (ε) is calculated from Beer's law. It can be seen that ε values of compounds **1–4** at maxima absorption wavelength (λ_{max}) are in the range $(1.3–5.1) \times 10^4/M^{-1}cm^{-1}$ comparable to that of Al complexes containing the **BTP** derivatives.[9] Interestingly, Mg complex **4** provides a ~2-fold higher ε value than the analogous Zn complex **3**. In solution, free ligand **1** shows a weak emission band at λ_{max} = 505 nm, whereas complexes **2–4** exhibit the stronger emission bands with λ_{max} ranging from 478 to 500 nm (Fig. 6). On the basis of the previous studies reported in the literature,[10] the observed luminescence of the complexes can be attributed to π*–π transitions occurring in their amino–BTP ligands. For the same concentration, the emission intensities of complexes **2–4** have the order **4** > **2** > **3**, likely because of the stronger rigidity of the ligands resulting from the better bonding with the Mg atom. To investigate the quantitative characterization of the PL intensity, the quantum yields of compounds **1–4** in solution are determined by using quinine sulfate in 0.1 M sulfuric acid as a standard. As shown in Table 1, the quantum yields of

Table 1 Optical properties of ligand **1** and complexes **2–4** in CH_2Cl_2 and the solid state

		Absorption			Emission		
Compound	Conditions (25 °C)	λ_{max} (nm)	ε ($M^{-1}cm^{-1}$)[a]	λ_{ex} (nm)	λ_{max} (nm)	Quantum yields ϕ[b]	Bandwidth at half-height (nm)
1	CH_2Cl_2	289	13480	289	505	0.035	104
	solid	346	—	450	505	—	78
2	CH_2Cl_2	276	15460	290	478	0.071	89
	solid	349	—	433	520	—	85
3	CH_2Cl_2	248	28620	285	500	0.056	108
	solid	365	—	441	517	—	76
4	CH_2Cl_2	243	51320	300	500	0.072	92
	solid	363	—	435	510	—	93

[a] Absorption coefficient was determined at λ_{max} in CH_2Cl_2. [b] Determined by using quinine sulfate in 0.1 M sulfuric acid as a standard ($\phi = 0.577$).

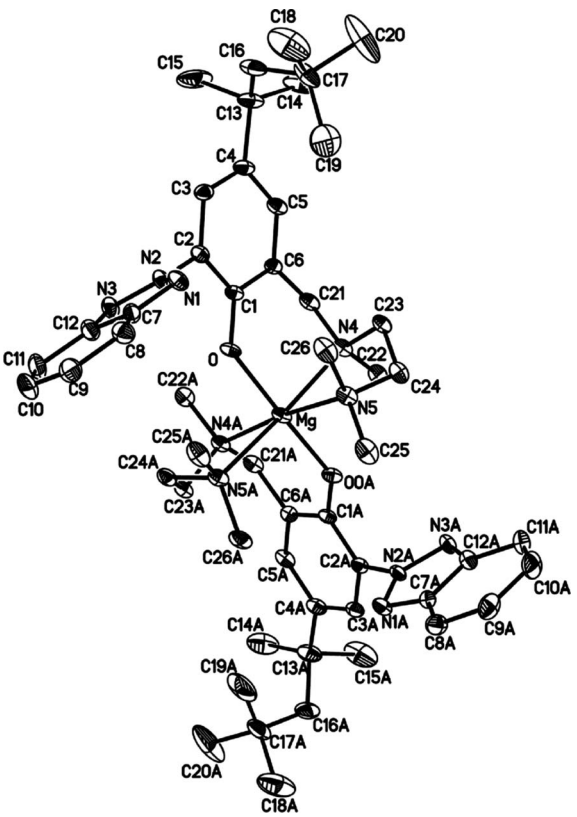

Fig. 5 ORTEP drawing of complex **4** with probability ellipsoids drawn at the 30% level. Hydrogen atoms are omitted for clarity. Selected bond lengths (Å) and angles (deg): Mg–O 1.929(3), Mg–N(4) 2.346(3), Mg–N(5) 2.314(3), O–Mg–O(0A) 171.47(17), O–Mg–N(5) 95.69(11), O–Mg–N(5A) 89.95(11), N(5A)–Mg–N(5) 97.38(16), O–Mg–N(4) 86.09(11), O(0A)–Mg–N(4) 88.74(11), N(5A)–Mg–N(4) 174.16(12), N(5)–Mg–N(4) 78.77(10), N(5A)–Mg–N(4) 174.16(12), N(4)–Mg–N(4A) 105.41(15).

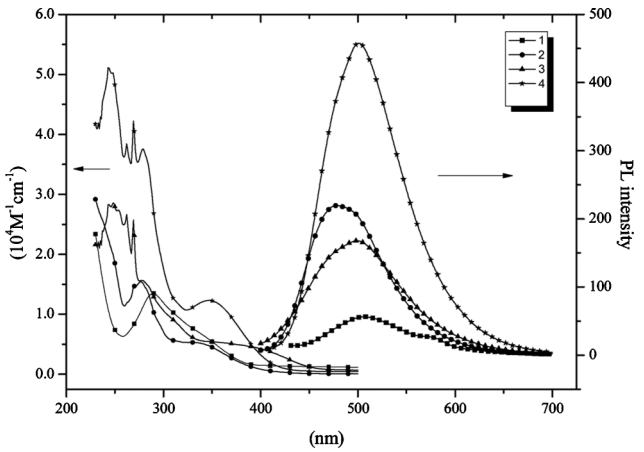

Fig. 6 UV-vis absorption spectra (left) and PL emission spectra (right) of **1–4** in CH_2Cl_2.

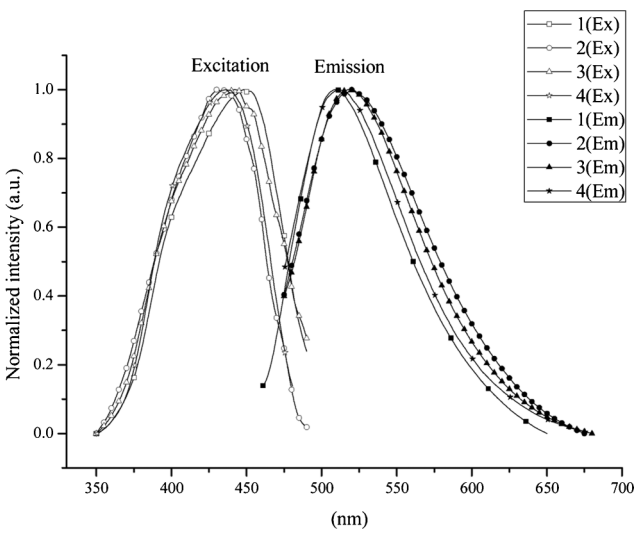

Fig. 7 Emission spectra of compounds **1–4** in the solid state.

complexes **2–4** are low in CH_2Cl_2 and whose values are in a range of 0.056–0.072.

The emission spectra of compounds **1–4** in the solid state are shown in Fig. 7. All complexes **2–4** emit bright green fluorescence when excited at the appropriate wavelength and possess a relatively narrow band (bandwidth at half-height = 85, 76 and 93 nm) with λ_{max} = 520, 517 and 510 nm in the solid state. The emission maxima of complexes **2–4** in the solid state display a slight redshift compared with the corresponding emission maximum of the free ligand **1**, which is probably caused by lowering the energy gap between π^* and π of the ligand owing to the coordination of the ligand to the metal center.[11]

Table 2 ROP of lactide (LA) catalyzed by complexes **2–4** in the presence of 9-AnOH

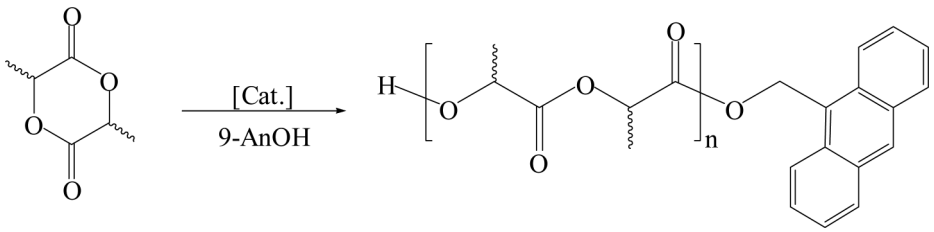

Entry	Cat.	$[LA]_0/[Cat.]_0/[9\text{-AnOH}]_0$	t (h)	Conv. (%)[e]	Mn (calcd.)[f]	Mn (obsd.)[g]	Mn (NMR)[h]	PDI[g]	P_m[i]
1[a]	**2**	100/1/1	3	99	14600	21800 (12600)	17 000	1.13	—[j]
2[a]	**3**	100/1/1	10	97	14200	22000 (12800)	16 300	1.07	—[j]
3[a]	**2**	25/1/1	3	99	3800	4600 (2700)	4000	1.20	—[j]
4[a]	**2**	50/1/1	3	99	7400	9200 (5300)	7900	1.18	—[j]
5[a]	**2**	200/1/1	3	99	29100	37000 (21500)	30 200	1.06	—[j]
6[a]	**4**	100/1/1	20	61	9000	12600 (7300)	8100	1.06	—[j]
7[b]	**2**	100/1/1	3	92	13500	14500 (8400)	15 100	1.05	0.51
8[c]	**2**	100/1/1	8	94	13800	10700 (6200)	17 000	1.16	0.59
9[d]	**2**	100/1/1	14	95	13900	12200 (7100)	17 400	1.41	0.57

[a] L-LA as the monomer, 0.1 mmol complexes, 10 mL CH_2Cl_2, 30 °C. [b] rac-LA as the monomer, 0.1 mmol complexes, 10 mL CH_2Cl_2, 30 °C. [c] rac-LA as the monomer, 0.1 mmol complexes, 10 mL THF, 30 °C. [d] rac-LA as the monomer, 0.1 mmol complexes, 15 mL THF, 30 °C. [e] Obtained from ^{1}H NMR determination. [f] Calculated from the molecular weight of lactide times $[LA]_0/[9\text{-AnOH}]_0$ times conversion yield plus the molecular weight of 9-AnOH. [g] Obtained from GPC analysis and calibrated by polystyrene standard. Values in parentheses are the values obtained from GPC times 0.58.[15] [h] Obtained from ^{1}H NMR analysis. [i] P_m is the probability of *meso* linkages between monomer units and is determined from the methine region of the homonuclear decoupled ^{1}H NMR spectrum. [j] Not determined.

ROP of lactides

Based on lactone polymerizations catalyzed by bis(benzotriazole-phenolate) Al complexes[5a] and mono(benzotriazole-phenoxide) Zn-Et derivatives,[5b] the single active-site zinc complexes supported by the ^{C8NN}**BTP**$^-$ ligand have the potential to behave as catalysts toward the lactide (LA) polymerization in the presence of 9-anthracenemethanol (9-AnOH). Representative results of the polymerizations of LA under varied conditions are depicted in Table 2. Similar conditions following our previous studies[12] were first applied to test the catalytic activities of L-LA polymerizations using **2**/9-AnOH as the catalytic system under a dry N_2 atmosphere. Optimized conditions were a zinc catalyst concentration of 0.01 M with 9-AnOH (1 molar equiv.) in CH_2Cl_2 (10 mL) at 30 °C. Experimental results indicated that Zn complexes displayed an effective activity and a controlled character. Mono-adduct complex **2** exhibits efficient activity within 3 h, whereas bis-adduct complex **3** can reach a similar conversion, but with durations up to 10 h (Table 2, entries 1–2). Consequently, in the polymerizations catalyzed by **2**, the "controlled" character was systematically examined under optimized conditions (Table 2, entries 1, 3–5). The conversion yields go to completion within 3 h with the ratio $[L\text{-LA}]_0/[9\text{-AnOH}]_0$ in a range of 25–200. The number-average molecular weight (M_n determined from ^{1}H NMR) of the produced polymers is close to the molecular weight calculated from the molar ratio of L-LA to 9-AnOH. As illustrated in Fig. 8, a linear relationship between the number-average molecular weight (M_n) and $[L\text{-LA}]_0/[9\text{-AnOH}]_0$ as well as narrow polydispersity indices (PDI = 1.06–1.20) demonstrates the "controlled" character of the polymerization. The ^{1}H NMR spectrum shows that the poly(L-lactide) (PLLA) chain is capped by one 9-anthracenemethyl ester and one hydroxyl chain end, which is the same as that reported in our previous studies.[5a] In comparison, Mg complex **4** reveals a poor activity (conversion = 61%, 20 h) but a similar control of molecular weight distribution toward the ROP of L-LA (Table 2, entry 6) under the optimal conditions of complex **2**.

The physical and degradation properties of PLA are known to be dependent on the microstructure of PLA.[13] As a result, polymerizations of rac-LA and their stereoselectivities catalyzed by Zn complex **2** are investigated. The catalytic activity and the controlled character are not drastically affected while rac-LA is employed as the monomer (Table 2, entry 7). According to the homonuclear decoupled ^{1}H NMR spectrum at the methine region, PLA is enriched in the "mmm" tetrad, suggesting isotactic predominance with $P_m > 0.50$. It was also found that the P_m value can be improved under different solvents in the ROP of rac-LA.[14] For instance, a virtually atactic polymer ($P_m = 0.51$) is afforded at 30 °C in CH_2Cl_2, whereas a higher isotactic selectivity ($P_m = 0.59$) is achieved at 30 °C in THF (Table 2, entry 8, Fig. 9).

Conclusions

Three new mononuclear complexes of the N,N,O-tridentate ^{C8NN}**BTP** ligand have been synthesized and fully characterized by spectroscopic studies as well as X-ray single crystal structural determinations. On the basis of PL measurements, Mg complex **4** emits the brightest green fluorescence under the same concentration of CH_2Cl_2 solution among these complexes. Polymerizations of L-LA and rac-LA catalyzed by Zn complex **2** in the presence of 9-anthracenemethanol exhibit efficient activities with good molecular weight control and give PLAs with narrow molecular weight distributions (PDI $\leqq$ 1.20). The stereoselectivity of rac-LA polymerization also has been demonstrated to afford a slightly isotactic preference ($P_m = 0.59$) in THF.

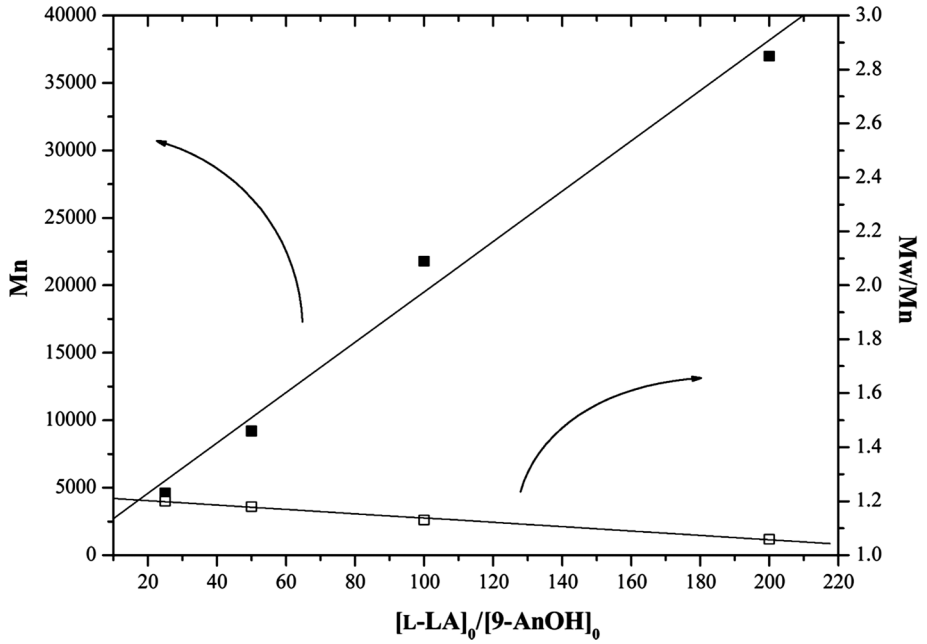

Fig. 8 Polymerization of L-LA catalyzed by **2** in CH_2Cl_2 (10 mL) at 30 °C. The relationship between M_n(■)PDI(□) of the polymer and the initial molar ratio $[L\text{-}LA]_0/[9\text{-}AnOH]_0$ is shown.

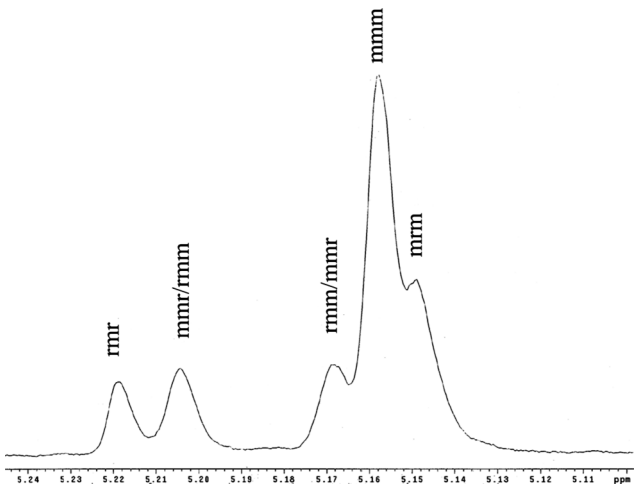

Fig. 9 Homonuclear decoupled ^{1}H NMR spectrum of the methine region of isotactic enriched PLA prepared from rac-LA with **2** in THF at 30 °C for 8 h (400 MHz, $CDCl_3$).

Experimental

General conditions

All manipulations were carried out under a dry nitrogen atmosphere. Solvents and reagents were dried by refluxing for at least 24 h over sodium/benzophenone (hexane, toluene, tetrahydrofuran (THF)), or over phosphorus pentoxide (CH_2Cl_2). Deuterated solvents were dried over 4 Å molecular sieves. L-Lactide and rac-lactide were recrystallized from a toluene solution prior to use. Mg^nBu_2 (1.0 M in heptane), $ZnEt_2$ (1.0 M in hexane), 2-(2*H*-benzotriazol-2-yl)-4-(2,4,4-trimethylpentan-2-yl)phenol (^{C8}**BTP-H**), N,N,N-trimethylethylene-diamine, paraformaldehyde and 9-anthracene-methanol (9-AnOH) were purchased and used without further purification. ^{1}H NMR and ^{13}C NMR spectra were recorded on Bruker Aveance (300 and 400 MHz) spectrometer with chemical shifts given in parts per million from the peak of internal TMS. Microanalyses were performed using a Heraeus CHN-*O*-RAPID instrument. Gel permeation chromatography (GPC) measurements were performed on a Jasco PU-2080 plus system equipped with a RI-2031 detector using THF (HPLC grade) as an eluent. The chromatographic column was Phenomenex Phenogel 5 μ 103 Å and the calibration curve used to calculate M_n (GPC) was produced from polystyrene standards. The GPC results were calculated using the Scientific Information Service Corporation (SISC) chromatography data solution 3.1 edition. UV/Vis absorption spectra were taken on an Evolution 201 UV-Visible spectrophotometer. Fluorescent measurements were recorded with a Hitachi F-4500.

Synthesis of ^{C8NN}BTP–H ligand (1)

To a mixture of paraformaldehyde (1.20 g, 40.0 mmol) and N,N,N-trimethylethylenediamine (5.20 mL, 40.0 mmol) was added 2-(2*H*-benzotriazol-2-yl)-4-(2,4,4-trimethylpentan-2-yl)phenol (3.23 g, 10.0 mmol). The resulting mixture was heated under reflux at 130 °C for 2 days and then dried under reduced pressure to yield the oil residue. The residue was extracted with ethyl acetate (3 × 50 ml) and the organic layers were dried over $MgSO_4$. The final solution was removed from the solvent under vacuum to give pale yellow solids. Yield: 3.10 g (71%). Anal. calc. for $C_{26}H_{39}N_5O$: N, 16.00; C, 71.36; H, 8.98. Found: N, 16.00; C, 71.28; H, 9.17%. Yellow crystals were obtained from the saturated hexane solution. ^{1}H NMR ($CDCl_3$, ppm): δ 7.97 (2H, m, Ar–*H*), 7.80 (1H, d, Ar–*H*), 7.42 (2H, m, Ar–*H*), 7.21 (1H, d, Ar–*H*), 3.78 (2H, s, CH_2), 2.62 (2H, t, CH_2), 2.51 (2H, t, CH_2), 2.32 (3H, s, CH_3), 2.20 (6H, s, $N(CH_3)_2$), 1.74 (2H, s, CH_2), 1.39 (6H, s, $C(CH_3)_2$), 0.75 (9H, s, $C(CH_3)_3$). ^{13}C NMR ($CDCl_3$, ppm): δ 148.64, 144.07,

140.63, 128.40, 127.11, 126.62, 124.54, 121.82, 118.09 (*Ar*), 59.39 (CH_2), 56.79 (CH_2), 54.74 (CH_2), 45.52 (CH_3), 42.01 (CH_3), 37.97 ($C(CH_3)_2$), 32.31 ($C(CH_3)_3$), 31.79 ($C(CH_3)_2$), 31.47 ($C(CH_3)_3$).

Synthesis of complex [(^{C8NN}BTP)ZnEt] (2)

To an ice cold solution (0 °C) of ^{C8NN}**BTP–H** (0.44 g, 1.0 mmol) in toluene (30 mL) was slowly added $ZnEt_2$ (1.2 mL, 1.0 M in hexene, 1.2 mmol). The mixture was stirred at room temperature for 4 h and was removed from the volatile components *in vacuo*. The residue was washed with hexane twice (2 × 15 mL) and the resulting precipitate was collected by filtration and then dried under vacuum to give yellow solids. Yield: 0.35 g (67%). Anal. calc. for $C_{28}H_{43}N_5OZn$: N, 13.19; C, 63.33; H, 8.16. Found: N, 13.19; C, 63.47; H, 8.06%. Yellow crystals were obtained from the saturated Et_2O solution. ^{1}H NMR ($CDCl_3$,ppm): δ 7.96 (2H, m, Ar–*H*), 7.40 (1H, d, Ar–*H*), 7.37 (2H, m, Ar–*H*), 7.07 (1H, d, Ar–*H*), 4.26 (1H, d, CH_2), 3.31 (1H, d, CH_2), 2.85 (1H, t, CH_2), 2.57 (3H, s, NCH_3), 2.46 (1H, t, CH_2), 2.29 (3H, s, NCH_3), 2.05 (3H, s, NCH_3), 2.31 (2H, m, CH_2), 1.69 (2H, s, CH_2), 1.32 (6H, s, $C(CH_3)_2$), 1.15 (3H, t, CH_2CH_3), 0.76 (9H, s, $C(CH_3)_3$), 0.06 (2H, q, CH_2CH_3). ^{13}C NMR ($CDCl_3$, ppm): δ 159.37, 144.61, 134.12, 131.49, 130.49, 125.51, 124.20, 118.43 (*Ar*), 62.82 (CH_2), 57.63 (CH_2), 56.94 (CH_2), 51.67 (CH_2), 47.49 (CH_3), 46.47 (CH_3), 44.85 (CH_3), 37.60 ($C(CH_3)_2$), 32.44 ($C(CH_3)_3$), 31.92 ($C(CH_3)_2$), 31.55 ($C(CH_3)_3$), 13.23 ($ZnCH_2CH_3$), –4.10 ($ZnCH_2CH_3$).

Synthesis of complex [(^{C8NN}BTP)$_2$Zn] (3)

To an ice cold solution (0 °C) of ^{C8NN}**BTP-H** (0.88 g, 2.0 mmol) in toluene (30 mL) was slowly added $ZnEt_2$ (1.0 mL, 1.0 mmol). The mixture was stirred at 50 °C for 8 h, and the volatile components were removed *in vacuo*. The residue was washed with hexane twice and the resulting precipitate was collected by filtration and then dried under vacuum to give yellow solids. Yield: 0.65 g (69%). Anal. calc. for $C_{52}H_{76}N_{10}O_2Zn$: N, 14.92; C, 66.54; H, 8.16%. Found: N, 14.65; C, 66.40; H, 8.05%. Pale yellow crystals were grown from the saturated Et_2O solution. ^{1}H NMR (0 °C, d_8-toluene, ppm): δ 7.85–7.83 (4H, m, Ar–*H*), 7.56 (2H, s, Ar–*H*), 7.11–7.09 (4H, m, Ar–*H*), 7.02 (2H, s, Ar–*H*), 4.13 (2H, d, CH_2), 3.11 (2H, t, NCH_2), 2.89–2.85 (4H, m, NCH_2), 2.28 (6H, s, NCH_3), 1.67 (4H, s, CH_2), 1.49–1.26 (20H, m, NCH_3 & $C(CH_3)_2$ & NCH_2), 1.03 (2H, d, NCH_2), 0.98–0.86 (24 H, m, $C(CH_3)_3$ & NCH_3).

Synthesis of complex [(^{C8NN}BTP)$_2$Mg] (4)

To an ice cold solution (0 °C) of ^{C8NN}**BTP-H** (0.88 g, 2.0 mmol) in toluene (30 mL) was slowly added Mg^nBu_2 (1.0 mL, 1.0 M in heptane, 1.0 mmol). The mixture was stirred at room temperature for 8 h, and the volatile components were removed *in vacuo*. The residue was washed with hexane twice and the resulting precipitate was collected by filtration and then dried under vacuum to give yellow solids. Yield: 0.70 g (80%). Anal. calc. for $C_{52}H_{76}N_{10}O_2Mg$: N, 15.61; C, 69.59; H, 8.53%. Found: N, 16.12; C, 69.08; H, 8.30%. Pale yellow crystals were crystallized from the saturated Et_2O solution. ^{1}H NMR (20 °C, d_8-toluene, ppm): δ 7.84–7.81 (4H, m, Ar–*H*), 7.56 (2H, s, Ar–*H*), 7.10–7.07 (4H, m, Ar–*H*), 7.06 (2H, s, Ar–*H*), 3.98 (2H, d, CH_2), 3.05 (2H, t, NCH_2), 2.87–2.79 (4H, m, NCH_2), 2.24 (6H, s, NCH_3), 1.68 (4H, s, CH_2), 1.52 (6H, s, NCH_3), 1.38 (2H, t, NCH_2), 1.37, 1.34 (12H, d, $C(CH_3)_2$), 1.04 (2H, d, NCH_2), 1.02 (6H, s, NCH_3), 0.86 (18H, s, $C(CH_3)_3$). ^{13}C NMR ($CDCl_3$, ppm): δ 148.38, 143.81, 140.34, 128.25, 126.85, 124.49, 121.50, 117.85 (*Ar*), 58.97 (CH_2), 56.56 (CH_2), 54.46 (CH_2), 45.29 (CH_3), 41.82 (CH_3), 37.75 ($C(CH_3)_2$), 32.10 ($C(CH_3)_3$), 31.62 ($C(CH_3)_2$), 31.31 ($C(CH_3)_3$).

Polymerization of lactide catalyzed by zinc bis(amine) benzotriazole phenoxide complex 2

A typical polymerization procedure was exemplified by the synthesis of PLLA-200 (the number 200 indicates the $[L\text{-LA}]_0/[9\text{-AnOH}]_0$ ratio). Polymerizations were carried out under a dry nitrogen atmosphere. To a solution of [(^{C8NN}**BTP**)**ZnEt**] (**2**) (0.053 g, 0.1 mmol) and 9-AnOH (0.020 g, 0.1 mmol) in CH_2Cl_2 (3 mL) was

Table 3 Crystallographic data of complexes **1–4**

	1	**2**	**3**	**4**
Empirical formula	$C_{26}H_{39}N_5O$	$C_{28}H_{43}N_5OZn$	$C_{52}H_{76}N_{10}O_2Zn$	$C_{52}H_{76}MgN_{10}O_2$
Formula weight	437.62	531.0	938.60	897.54
T/K	173(2)	173(2)	100(2)	100(2)
Crystal system	Triclinic	Monoclinic	Monoclinic	Monoclinic
Space group	$P\bar{1}$	$P2_1/c$	$C2/c$	$C2/c$
a/Å	7.7158(2)	11.4457(2)	23.1996(4)	23.2246(16)
b/Å	13.8315(3)	18.0495(3)	8.3354(2)	8.3575(5)
c/Å	13.9203(3)	13.8545(2)	27.7046(5)	27.7372(16)
α (°)	60.8960(10)	90	90	90
β (°)	75.1230(10)	104.9120(10)	105.7270(10)	105.400(4)
γ (°)	82.3810(10)	90	90	90
V/Å^3	1254.45(5)	2765.80(8)	5156.90(18)	5190.5(6)
Z	2	4	4	4
D_c/Mg m^{-3}	1.159	1.275	1.209	1.149
μ(Mo-Kα)/mm^{-1}	0.072	0.917	0.525	0.083
F(000)	476	1136	2016	1944
Reflections collected	22240	26055	23426	22322
No. of parameters	301	325	302	303
Indep. reflns (R_{int})	6228 (0.0271)	6858 (0.0214)	6389 (0.0324)	6250 (0.0536)
$R_1[I > 2\sigma(I)]$	0.0514	0.0491	0.0373	0.1005
wR_2 $[I > 2\sigma(I)]$	0.1308	0.1328	0.0948	0.2106
Goodness-of-fit on F^2	1.095	1.052	1.037	1.133

rapidly stirred at 30 °C. After 5 min, L-lactide (2.88 g, 20.0 mmol) in CH_2Cl_2 (7 mL) were added to the activated species, and the reaction mixture was stirred at 30 °C for 3 h. The conversion yield (99%) of PLLA-200 was analyzed by ^{1}H NMR spectroscopic analysis. After the reaction was quenched by the addition of excess water (0.5 mL), the polymer was precipitated into hexane (100 mL). The final polymer was then dissolved in THF (20 mL) and purified upon precipitation again in MeOH (150 mL), collected and dried under vacuum. Yield: 2.76 g (96%).

X-ray crystallographic studies

Suitable crystals of complex **1–4** were mounted onto glass fiber using perfluoropolyether oil and cooled rapidly in a stream of cold nitrogen gas to collect diffraction data at 173 K or 100 K using Bruker APEX2 diffractometer. Intensity data were collected in 1350 frames with increasing *w* (width of 0.5° per frame). The absorption correction was based on the symmetry-equivalent reflections using SADABS program.[16] The space group determination was based on a check of the Laue symmetry and systematic absence, and was confirmed using the structure solution. The structures were solved with direct methods using a SHELXTL package.[17] All non-H atoms were located from successive Fourier maps, and hydrogen atoms were refined using a riding model. Anisotropic thermal parameters were used for all non-H atoms, and fixed isotropic parameters were used for H-atoms. Crystallographic data of complexes **1–4** are summarized in Table 3.

Acknowledgements

We gratefully acknowledge financial support from the National Science Council, Taiwan (NSC99-2113-M-033-007-MY2). We also thank Professor Pi-Tai Chou and Dr Ching-Yen Wei for valuable discussions of PL quantitative characterization.

References

1 (*a*) B. J. O'Keefe, M. A. Hillmyer and W. B. Tolman, *J. Chem. Soc., Dalton Trans.*, 2001, 2215–2224; (*b*) A. C. Albertsson and I. K. Varma, *Biomacromolecules*, 2003, **4**, 1466–1486; (*c*) O. Dechy-Cabaret, B. Martin-Vaca and D. Bourissou, *Chem. Rev.*, 2004, **104**, 6147–6176; (*d*) J. Wu, T.-L. Yu, C.-T. Chen and C.-C. Lin, *Coord. Chem. Rev.*, 2006, **250**, 602–626; (*e*) C. A. Wheaton, P. G. Hayes and B. J. Ireland, *Dalton Trans.*, 2009, 4832–4846.

2 (*a*) W. Gao, D. Cui, X. Liu, Y. Zhang and Y. Mu, *Organometallics*, 2008, **27**, 5889–5893; (*b*) W. Yao, Y. Mu, A. Gao, W. Gao and L. Ye, *Dalton Trans.*, 2008, 3199–3206; (*c*) Y.-H. Tsai, C.-H. Lin, C.-C. Lin and B.-T. Ko, *J. Polym. Sci., Part A: Polym. Chem.*, 2009, **47**, 4927–4936; (*d*) Y.-C. Liu, C.-H. Lin, B.-T. Ko and R.-M. Ho, *J. Polym. Sci., Part A: Polym. Chem.*, 2010, **48**, 5339–5347.

3 (*a*) C. K. Williams, N. R. Brooks, M. A. Hillmyer and W. B. Tolman, *Chem. Commun.*, 2002, 2132–2133; (*b*) C. K. Williams, L. E. Breyfogle, S. K. Choi, W. Nam, V. G. Jr. Young, M. A. Hillmyer and W. B. Tolman, *J. Am. Chem. Soc.*, 2003, **125**, 11350–11359; (*c*) L. M. Alcazar-Roman, B. J. O'Keefe, M. A. Hillmyer and W. B. Tolman, *Dalton Trans.*, 2003, 3082–3087; (*d*) C.-T. Chen, C.-A. Huang and B.-H Huang, *Dalton Trans.*, 2003, 3799–3803; (*e*) C.-T. Chen, C.-A. Huang and B.-H. Huang, *Macromolecules*, 2004, **37**, 7968–7973; (*f*) L. E. Breyfogle, C. K. Williams, V. G. Jr. Young, M. A. Hillmyer and W. B. Tolman, *Dalton Trans.*, 2006, 928–936; (*g*) A. Amgoune, C. M. Thomas, S. Ilinca, T. Roisnel and J.-F. Carpentier, *Angew. Chem., Int. Ed.*, 2006, **45**, 2782–2784; (*h*) J. Ejfler, S Szafert, K. Mierzwicki, L. B. Jerzykiewicz and P. Sobota, *Dalton Trans.*, 2008, 6556–6562; (*i*) C.-A. Huang, C.-L. Ho and C.-T. Chen, *Dalton Trans.*, 2008, 3502–3510; (*j*) N. Ajellal, M. Bouyahyi, A. Amgoune, C. M. Thomas, A. Bondon, I. Pillin, Y. Grohens and J.-F. Carpentier, *Macromolecules*, 2009, **42**, 987–993; (*k*) V. Poirier, T. Roisnel, J.-F. Carpentier and Y. Sarazin, *Dalton Trans.*, 2009, 9820–9827; (*l*) G. Labourdette, D. J. Lee, B. O. Patrick, M. B. Ezhova and P. Mehrkhodavandi, *Organometallics*, 2009, **28**, 1309–1319.

4 (*a*) H.-Y. Chen, H.-Y. Tang and C.-C. Lin, *Macromolecules*, 2006, **39**, 3745–3752; (*b*) W.-C. Hung, Y. Huang and C.-C. Lin, *J. Polym. Sci., Part A: Polym. Chem.*, 2008, **46**, 6466–6476; (*c*) W.-C. Hung and C.-C. Lin, *Inorg. Chem.*, 2009, **48**, 728–734.

5 (*a*) C.-Y. Li, C.-Y. Tsai, C.-H. Lin and B.-T. Ko, *Dalton Trans.*, 2011, 1880–1887; (*b*) Y.-E. Tai, C.-Y. Li, C.-H. Lin, Y.-C. Liu, B.-T. Ko and Y.-S. Sun, *J. Polym. Sci., Part A: Polym. Chem.*, 2011, **49**, 4027–4036.

6 (*a*) J.-Y. Li, Y.-C. Liu, C.-H. Lin and B.-T. Ko, *Acta Crystallogr., Sect. E: Struct. Rep. Online*, 2009, **E65**, o2475; (*b*) C.-H. Li, J.-K. Su, C.-Y. Li and B.-T. Ko, *Acta Crystallogr., Sect. E: Struct. Rep. Online*, 2010, **E66**, o2825.

7 J.-Y. Li, C.-Y. Li, W.-J. Tai, C.-H. Lin and B.-T. Ko, *Inorg. Chem. Commun.*, 2011, **14**, 1140–1144.

8 J. Rosevear and J. F. K. Wilshire, *Aust. J. Chem.*, 1985, **38**, 1163–1176.

9 J. Lee, S. H. Kim, K. M. Lee, K. Y. Hwang, H. Kim, J. O. Huh, D. J. Kim, Y. S. Lee, Y. Do and Y. Kim, *Organometallics*, 2010, **29**, 347–353.

10 (*a*) W. Y. Yang, H. Schmider, Q. D. Wu, Y. S. Zhang and S. Wang, *Inorg. Chem.*, 2000, **39**, 2397–2404; (*b*) Q. G. Wu, J. A. Lavigue, Y. Tao, M. D'Iorio and S. Wang, *Inorg. Chem.*, 2000, **39**, 5248–5254; (*c*) X. Liu, W. Gao, Y. Mu, G.-H. Li, L. Ye, H. Xia, Y. Ren and S.-H. Feng, *Organometallics*, 2005, **24**, 1614–1619; (*d*) Q. Su, W. Gao, Q.-L. Wu, L. Ye, G.-H. Li and Y. Mu, *Eur. J. Inorg. Chem.*, 2007, 4168–4175.

11 (*a*) D. Rendell, (Ed.), *Fluorescence and Phosphorescence*, Wiley, New York, 1987; (*b*) H. Yersin, A. Vogler, (ed.), (*Photochemistry and Photophysics of Coordination Compounds*, Springer, Berlin, 1987; (*c*) A. W. Adamson, P. D. Fleischauer, (ed.), (*Concepts of Inorganic Photochemistry*, Wiley, New York, 1975; (*d*) N. I. Nijegorodov and W. S. Downey, *J. Phys. Chem.*, 1994, **98**, 5639–5643.

12 (*a*) C.-Y. Tsai, C.-Y. Li, C.-H. Lin, B.-H. Huang and B.-T. Ko, *Inorg. Chem. Commun.*, 2011, **14**, 271–275; (*b*) C.-H. Wang, C.-Y. Li, C.-H. Lin, Y.-C. Liu and B.-T. Ko, *Inorg. Chem. Commun.*, 2011, **14**, 1456–1460.

13 (*a*) H. Tsujit and Y. Ikada, *Macromolecules*, 1993, **26**, 6918–6926; (*b*) R. T. MacDonald, S. P. McCarthy and R. A. Gross, *Macromolecules*, 1996, **29**, 7356–7361; (*c*) J. Huang, M. S. Lisowski, J. Runt, E. S. Hall, R. T. Kean, N. Buehler and J. S. Lin, *Macromolecules*, 1998, **31**, 2593–2599; (*d*) J. R. Sarasua, R. E. Prud'homme, M. Wisniewski, A. L. Borgne and N. Spassky, *Macromolecules*, 1998, **31**, 3895–2905; (*e*) R. E. Drumright, P. R. Gruber and D. E. Henton, *Adv. Mater.*, 2000, **12**, 1841–1846.

14 (*a*) J.-C. Wu, B.-H. Huang, M.-L. Hsueh, S.-L. Lai and C.-C. Lin, *Polymer*, 2005, **46**, 9784–9792; (*b*) Y. Huang, W.-C. Hung, M.-Y. Liao, T.-E. Tsai, Y.-L. Peng and C.-C. Lin, *J. Polym. Sci., Part A: Polym. Chem.*, 2008, **46**, 6466–647.

15 (*a*) J. Baran, A. Duda, A. Kowalski, R. Szymanski and S. Penczek, *Macromol. Rapid Commun.*, 1997, **18**, 325–333The *M*n (GPC) value is multiplied by a factor of 0.58, giving the actual M_n of the polylactide, see: (*b*) T. Biela, A. Duda and S. Penczek, *Macromol. Symp.*, 2002, **183**, 1–10.

16 G. M. Sheldrick, *SADABS, Program for area detector absorption correction*, Institute for Inorganic Chemistry, University of Göttingen, Germany, 1996.

17 G. M. Sheldrick, *SHELXTL-97, Program for refinement of crystal structures*, University of Göttingen, Germany, 1997.